

Phase statistics approach to human ventricular fibrillationMing-Chya Wu,^{1,2,3,*} Eiichi Watanabe,^{4,†} Zbigniew R. Struzik,^{5,‡} Chin-Kun Hu,^{2,6,§} and Yoshiharu Yamamoto^{5,||}¹*Research Center for Adaptive Data Analysis, National Central University, Chungli 32001, Taiwan*²*Institute of Physics, Academia Sinica, Nankang, Taipei 11529, Taiwan*³*Department of Physics, National Central University, Chungli 32001, Taiwan*⁴*Division of Cardiology, Department of Internal Medicine, Fujita Health University School of Medicine, Toyoake, Aichi-Ken 470-1192, Japan*⁵*Educational Physiology Laboratory, Graduate School of Education, The University of Tokyo, Bunkyo-ku, Tokyo 113-0033, Japan*⁶*Center for Nonlinear and Complex Systems and Department of Physics, Chung Yuan Christian University, Chungli 32023, Taiwan*

(Received 27 July 2009; revised manuscript received 25 October 2009; published 20 November 2009)

Ventricular fibrillation (VF) is known to be the most dangerous cardiac arrhythmia, frequently leading to sudden cardiac death (SCD). During VF, cardiac output drops to nil and, unless the fibrillation is promptly halted, death usually ensues within minutes. While delivering life saving electrical shocks is a method of preventing SCD, it has been recognized that some, though not many, VF episodes are self-terminating, and understanding the mechanism of spontaneous defibrillation might provide newer therapeutic options for treatment of this otherwise fatal arrhythmia. Using the phase statistics approach, recently developed to study financial and physiological time series, here, we reveal the timing characteristics of transient features of ventricular tachyarrhythmia (mostly VF) electrocardiogram (ECG) and find that there are three distinct types of probability density function (PDF) of phase distributions: uniform (UF), concave (CC), and convex (CV). Our data show that VF patients with UF or CC types of PDF have approximately the same probability of survival and nonsurvival, while VF patients with CV type PDF have zero probability of survival, implying that their VF episodes are never self-terminating. Our results suggest that detailed phase statistics of human ECG data may be a key to understanding the mechanism of spontaneous defibrillation of fatal VF.

DOI: [10.1103/PhysRevE.80.051917](https://doi.org/10.1103/PhysRevE.80.051917)

PACS number(s): 87.19.Hh, 05.45.Tp

I. INTRODUCTION

In recent decades, methods of statistical physics have been widely used to study various complex time series and useful multiscale characteristics of the studied systems have been obtained. For example, detrended fluctuation analysis (DFA) [1], wavelet transform [2,3], and multiscale fluctuation probability density analysis [4,5], developed in statistical physics and nonlinear dynamics communities, have been used to measure properties in a wide range of phenomena, including the biological [1,6], physiological [5,7,8], geophysical [9,10], and financial [11–15]. While these methods address mainly multiscale amplitude properties the recently proposed empirical mode decomposition (EMD) [16] based approach [17–20] addresses phase properties in complex signals. The EMD was originally designed to obtain a relevant measure of the instantaneous frequency, related to the derivative of the phase, from nonlinear and nonstationary data. Due to its adaptive features and decompositions with different scales, it has been a useful tool for data analysis in both time and frequency domains [16]. However, it has rarely been used for the analysis of cardiac data. In the present paper, we demonstrate that phase statistics of heart beat signals can be used to study a yet unknown mechanism of spontaneous ter-

mination of fatal ventricular fibrillation (VF) in clinical settings.

Sudden cardiac death (SCD) is both a leading and a growing cause of death in the industrialized world. It is estimated that more than 3 million people die annually from SCD, with a survival rate of less than 1%. VF is identified as a primary cause of SCD, accounting for 75% to 85% of sudden deaths [21]. In the United States, the Centers for Disease Control recently estimated an annual incidence of 450 000 sudden deaths [22]. The magnitude of this problem can be understood by noting that SCD accounts for more deaths each year than the total number of deaths from AIDS, breast cancer, lung cancer, and stroke [23].

Automatic defibrillation by implantable cardioverter defibrillators (ICD) has become the gold standard therapy for patients at a high risk of ventricular tachyarrhythmias (VTA) [23], including VF. However, the overall benefit of ICD in terms of quality of life is diminished by the fear of shock, resulting in reduced daily activity levels, anxiety, and symptoms of depression [24,25]. Cost and other factors limit the widespread applicability of ICDs [26]. Furthermore, only 10% of sudden cardiac arrest victims are of a high-risk profile, and the challenge is, therefore, to improve the outcome of resuscitation in about 90% of patients who are not recognized as being at high risk before the event. A major breakthrough in improving results of cardiac resuscitation could come from developing an apparatus specifically geared toward minimizing the time between collapse and resuscitation [27]. The success of such a device is, however, dependent on minimizing false positive and low risk alarms. Research into the mechanism of VF is, therefore, of great clinical importance.

*mcwu@ncu.edu.tw

†enwatan@fujita-hu.ac.jp

‡zbigniew.struzik@p.u-tokyo.ac.jp

§huck@phys.sinica.edu.tw

||yamamoto@p.u-tokyo.ac.jp

Although VF usually is sustained and unrelenting in human subjects and is rarely self-terminating, it has been reported that some VF episodes are indeed self-terminating, and suggested that the understanding the mechanism of spontaneous defibrillation might provide therapeutic options for treatment of this otherwise fatal arrhythmia [28]. Furthermore, several mechanisms, such as the multiple wavelet mechanism [29] and the mother rotor hypothesis [30], have been shown to underlie the complex activation patterns of VF and have been demonstrated in various experimental models, while their relative roles in human VF have not been established. Here, we show that the lack of self-termination of VF is correlated with convexity in phase distribution patterns from the decomposition of ECG time series from VTA patients. More specifically, VTA can either be self-terminating or non-self-terminating, while the CV type VF is never self-terminating. Our study is generally based on observations, aimed to provide a criterion for modeling and as a reference for further animal experiments.

The rest of the paper is organized as follows. In the next section, we present the data source used in this study. The phase statistics approach is introduced in Sec. III. Our results and discussions are presented in Sec. IV. For conciseness and clarity, detailed illustrations of the results, mainly figures, are presented in the Appendix. Finally, we conclude briefly in Sec. V.

II. DATA

We analyzed the ECG data from patients who had VTA while undergoing 24-h Holter recording in the Fujita Health University Hospital. The study protocol was approved by the ethics committee of the institution. All the patients or their families provided informed written consent (Fujita Health University Hospital). We used CARDY2 two-channel Holter ECG recorders (Suzuken, Japan). The ECG signals were digitized at 125 Hz and 12 bits, and processed off-line using a personal computer equipped with software (Cardy Analyzer II, Suzuken, Japan). Dynamic range was 500 mV and 1 bit has a 20 μ V resolution power. The Holter system used 0.05 through 40 Hz signal via a bandpass pass filter to eliminate noise and baseline drift. We investigated ECGs of the 17 patients (age, 66 ± 18 years, mean \pm SD, male/female = 13/4), in whom 6 survived due to spontaneous termination, 10 died as a result of VF, and 1 died as a result of ventricular tachycardia (VT). VT was detected when at least 3 ventricular ectopic complexes occurred at a rate of at least 120 beats/min. VF was detected when the ventricular wave pattern became disorganized and grossly irregular [31]. A typical ECG data showing the transitions from sinus rhythm to VT and then to VF is shown in Fig. 1.

The baseline characteristics of the patients are summarized in Table I. The underlying heart diseases of these patients included ischemic heart disease ($n=10$), complete atrioventricular block ($n=3$), hypertension ($n=2$), and long-QT syndrome ($n=1$), and no cardiac disease was detected in one patient. Eleven recordings were made out-of-hospital and the other 6 were recorded during hospitalization due to heart failure or syncope. No patients received a car-

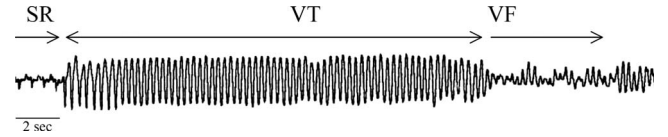


FIG. 1. A typical ECG recording, extracted from subject S_{03} , showing the transitions from sinus rhythm (SR) to VT and then to VF.

diac pacemaker or ICD at the time of Holter recording, and the basic cardiac rhythm was sinus rhythm in all the patients except patients with complete atrioventricular block (S_{04} , S_{07} , and S_{13}). These data were recorded by the CM5 lead (the bipolar V_5 lead) at the sampling frequency of 125 Hz, which is sufficiently high for typical frequencies of VF ranging from 3 to 20 Hz [32].

The low number of ECGs available is definitely a limitation to our study. We were, however, unable to increase this number as the actual records of the VF occurrence were extremely rare in spite of the prevalence.

III. PHASE STATISTICS APPROACH

The timing characteristics of transient features of nonstationary time series such as VF ECG records are best described with the concept of the instantaneous phase. For this purpose, here, we employ EMD to decompose time series “empirically” into a number of intrinsic mode functions (IMFs) [16], and calculate the instantaneous phases of these IMFs by the Hilbert transform. The EMD method has been developed on the assumption that any time series consists of simple intrinsic modes of oscillations [16]. The adaptive decomposition scheme explicitly utilizes the actual time series for the construction of the decomposition base rather than decomposing it into a prescribed set of base functions. The decomposition is achieved by iterative “sifting” processes for extracting modes by identification of local extremes and subtraction of local means [16]. The iterations are terminated by a criterion of convergence. For details of the sifting, reference is made to Refs. [16,18]. Following the procedure of EMD [16], we decompose a time series $x(t)$ into n IMFs c_i 's and a residue r_n , i.e.,

$$x(t) = \sum_{i=1}^n c_i(t) + r_n(t), \quad (1)$$

$$c_i(t) = r_{i-1}(t) - r_i(t). \quad (2)$$

For the purpose of illustration, we perform the EMD on the first VF time series of patient S_{05} in Table I. The stopping criterion is chosen as the number of points satisfying the condition of IMF in the data of c_i being less than 3. The time series is decomposed into 12 modes and we show the results c_1, c_2, \dots, c_5 in Fig. 2. Among the resultant IMFs, the first IMF c_1 has the highest frequency. The first four modes c_1, c_2, c_3 , and c_4 are essential components of the detailed structure of the original time series $x(t)$. In particular, c_3 contributes dominantly to the profile of $x(t)$.

The physical meanings of the IMFs obtained can be elucidated from the insights into the mechanisms of VF. During

TABLE I. Summary of VTA database and results of the present study.

Code	Age	Sex	Underlying disease ^a	Ventricular arrhythmia ^b	Outcome	VTA analysis time	Δt (sec) ^c	χ ^d	Pattern ^e
S_{01}	46	M	IHD	VT → VF	Dead	7:37:40-	9.324	0.044	CV
S_{02}	68	M	IHD	VF	Dead	22:59:51–23:01:31	100.992	0.096	CV
S_{03}	67	M	IHD	VT → VF	Dead	19:42:10-	405.000	-0.100	CC
S_{04}	97	F	CAVB	VT → VF		3:56:31–3:57:45	73.992	0.030	CV
				VT → VF		14:04:49–14:05:07	19.992	-0.094	CC
				VT → VF	Dead	21:38:56–21:40:19	82.992	-0.010	UF
S_{05}	80	M	IHD	VT → VF		10:32:03-	228.000	0.099	CV
				VT → VF		10:37:27–10:37:50	25.000	0.052	CV
				VT → VF		10:38:29–10:39:17	49.000	-0.093	CC
				VT → VF		10:39:54–10:40:33	40.000	0.075	CV
				VT → VF	Dead	11:05:58–11:09:30	213.000	0.068	CV
S_{06}	22	F	LQT	TdP		1:11:50–1:12:10	19.992	-0.094	CC
				VT → VF	Alive	3:44:07–3:46:01	113.992	0.006	UF
S_{07}	75	F	CAVB	VT → VF	Alive	14:53:00-	64.208	-0.006	UF
S_{08}	80	M	IHD	VT → VF	Dead	12:22:58–12:26:10	191.992	-0.041	CC
S_{09}	70	M	HTN	VT → VF	Alive	15:53:52–15:55:25	92.992	-0.039	CC
S_{10}	67	M	IHD	VT → VF	Dead	23:07:50–23:26:00	1089.992	0.052	CV
S_{11}	71	M	IHD	VT → VF		16:49:30–16:50:40	69.992	-0.045	CC
				VT → VF		00:24:05–0:25:40	94.992	-0.044	CC
				VT → VF		3:22:15–3:25:30	194.992	-0.082	CC
				VT → VF	Alive	6:05:10–6:07:50	159.992	-0.047	CC
S_{12}	66	M	IHD	VT → VF	Dead	12:38:31–12:52:40	848.992	0.023	UF
S_{13}	56	M	CAVB	TdP	Alive	20:01:38–20:02:08	29.992	-0.083	CC
S_{14}	88	M	IHD	VT	Dead	4:44:30-	114.992	0.005	UF
S_{15}	51	F	HTN	TdP	Alive	12:36:24–12:37:15	50.992	-0.021	UF
S_{16}	75	M	IHD	VT		14:47:40–15:13:45	1564.992	-0.044	CC
				VT → VF	Dead	15:50:10–16:09:00	1129.992	-0.016	UF
S_{17}	43	M	ND	VT → VF	Dead	18:41:06–18:50:38	492.800	-0.037	CC

^aIschemic heart disease (IHD); complete atrioventricular block (CAVB); long-QT (LQT) syndrome; hypertension (HTN); not detected (ND).
^bVT; (VF); torsades de pointes (TdP).

^c Δt is the available data time interval for analysis.

^d χ is defined in Eq. (8).

^eCC; CV; UF.

fibrillation, the coordinated contraction of the cardiac muscle is lost, and the mechanical pumping effectiveness of the heart fails as a result of the subsequent breakdown of the re-entrant wave into multiple drifting and meandering spiral waves [33–35]. In the (disorganized) state of VF, re-entrant waves continue to break into multispiral waves. Therefore, there are a number of re-entrant waves and spiral waves in cardiac tissue. The ECG signal is an average of their electric activities. As a result, IMF c_3 can be considered as a mean-field average of the variation of electric potential controlled by the re-entrant waves, while c_1 and c_2 describe higher-frequency fluctuations, reflecting the spatial and temporal dynamics of the multidrifting and meandering spiral waves. In other words, the existence of fluctuations of electric potential in the high frequency may serve as an index for the appearance of the multispiral waves. The measurements of such fluctuations can then be characterized by inhomogeneities (the clustering) of phases.

The instantaneous phase of the resultant IMFs can be calculated by using the Hilbert transform. For the k th mode, this is done by first calculating the conjugate pair of $c_k(t)$, i.e.,

$$y_k(t) = \frac{1}{\pi} P \int_{-\infty}^{\infty} \frac{c_k(t')}{t-t'} dt', \quad (3)$$

where P indicates the Cauchy principal value. With this definition, two functions $c_k(t)$ and $y_k(t)$ forming a complex conjugate pair define an analytic signal, and one can further define

$$c_k(t) + iy_k(t) = A_k(t)e^{i\phi_k(t)}, \quad (4)$$

with the amplitude $A_k(t)$ and the phase $\phi_k(t)$ defined by

$$A_k(t) = [c_k^2(t) + y_k^2(t)]^{1/2}, \quad (5)$$

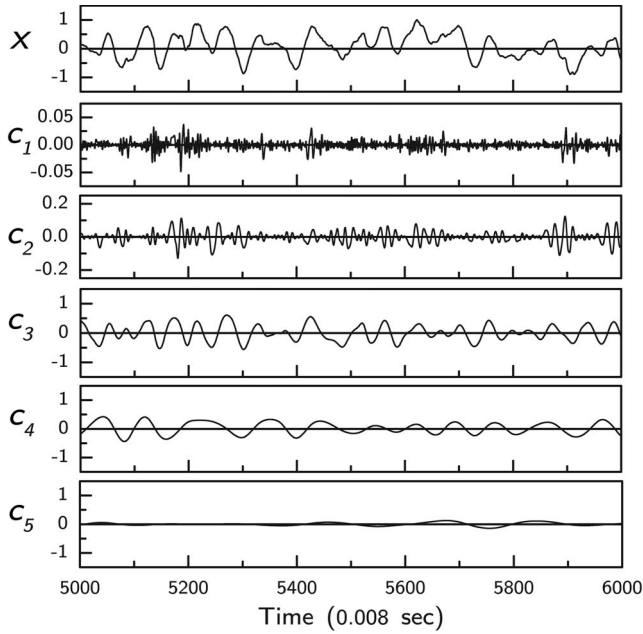


FIG. 2. Empirical mode decomposition for the VF time series of patient S_{05} .

$$\phi_k(t) = \tan^{-1} \left[\frac{y_k(t)}{c_k(t)} \right]. \quad (6)$$

Then, we can calculate the instantaneous phase by Eqs. (3) and (6) for the k th IMF. The phase variations of the first three IMFs c_1 , c_2 , and c_3 in Fig. 2 are shown in Fig. 3, and the corresponding phase histograms are shown in Fig. 4.

The statistics of the time series of phases, ranging from $-\pi$ to π , are characterized by calculating the probability density function (PDF) of phase distributions, which contain valuable information. In contrast to various types of phase distribution, the distributions of the amplitudes of all IMFs obey the simple Boltzmann distribution. The same property has also been observed in financial time series [17]. The first IMF c_1 has a distribution markedly different from those of c_2 and c_3 , while most higher order IMFs have a uniform distribution. We distinguish different basic morphological types (classes) of normalized histograms of the first IMF by using the following normalization condition:

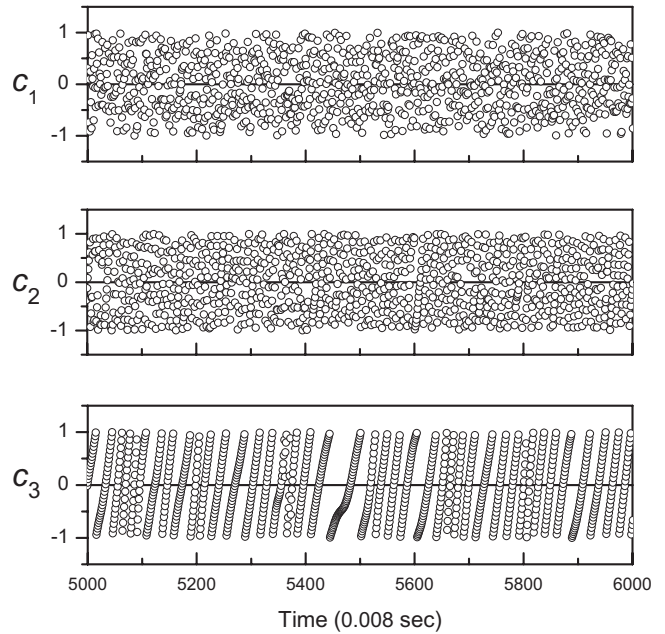


FIG. 3. The instantaneous phase for the first 3 IMFs c_1 , c_2 , and c_3 of the VF time series of S_{05} .

$$\int_{-\pi}^{\pi} P(\phi_k) d\phi_k = 1, \quad (7)$$

where P stands for the PDF. Let us consider a number of waves as shown in Fig. 5 for illustration.

For the sake of simplicity, we choose to consider constant amplitude functions, as this does not restrict the generality of phase distribution classes. For the time series of the uniform (UF) type phase distribution, the data points sampled have an equal probability of having a phase in $-\pi \leq \phi_1 \leq \pi$. In some other cases, data points located near the baseline contribute substantially to the phase distribution at $-\pi$ and π . This corresponds to the concave (CC) type phase distribution. In contrast, if there are more data points located near the peaks, there will be a higher distribution density in the range of -0.5π to 0.5π . This is the convex (CV) type distribution. In order to quantify the morphology of the phase distribution pattern, we define a measure χ ,

$$\chi = \langle P_1(\phi_1) \rangle - \langle P_2(\phi_1) \rangle, \quad (8)$$

where $\langle \dots \rangle$ denotes an average, $P_1(\phi_1)$ is the PDF for the instantaneous phase ϕ_1 of IMF c_1 in the range $-0.5\pi \leq \phi_1$

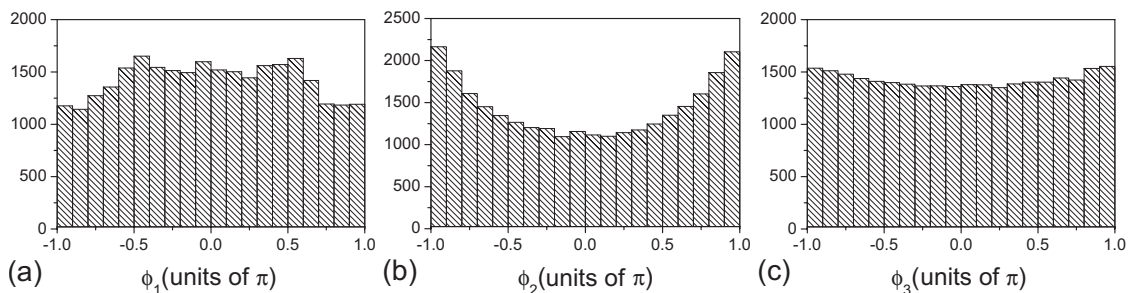


FIG. 4. Phase histograms for (a) the first IMF c_1 , (b) the second IMF c_2 , and (c) the third IMF c_3 of the VF of S_{05} (nonsurvivor).

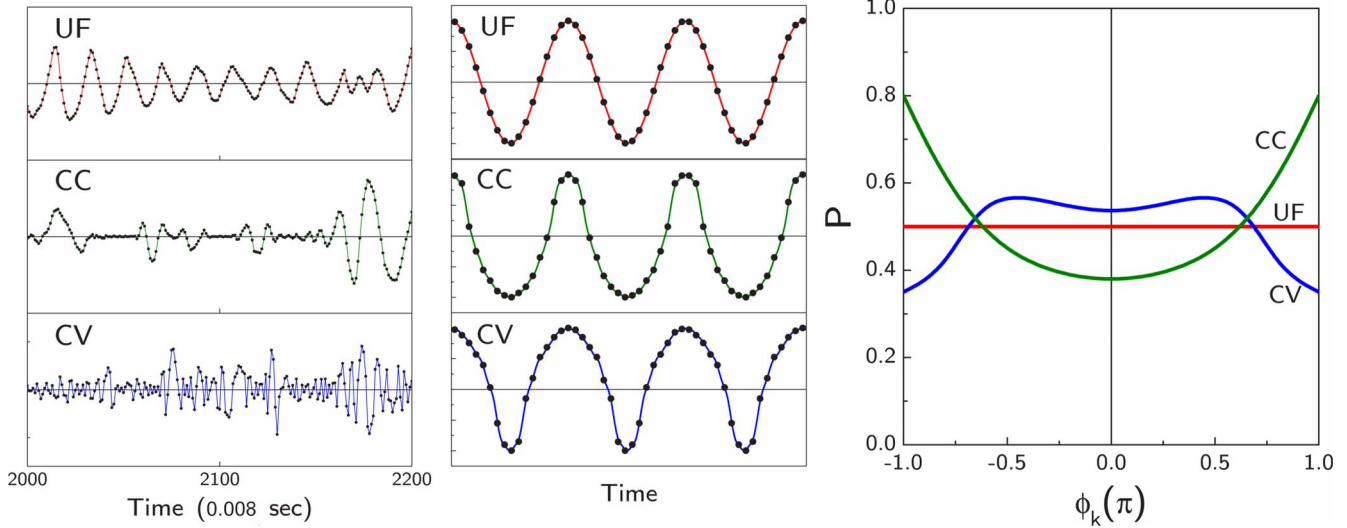


FIG. 5. (Color online) The first IMFs of real signals (left) and schematic drawings (middle) for three types of time series, and the corresponding (normalized) phase distribution patterns (right). The UF type real signal is taken from patient S_{07} ; the CC type is from patient S_{03} ; and the CV type is from patient S_{05} .

$\leq 0.5\pi$, and P_2 is for the phase in the range $-\pi \leq \phi_1 < -0.5\pi$ or $0.5\pi < \phi_1 \leq \pi$. More specifically, χ is a measure of the difference between the average of the PDFs of the phases located in the range $-0.5\pi \leq \phi_1 \leq 0.5\pi$ and the average of those not in this range. The three types of phase distribution patterns can then be quantitatively defined by

- (a) CV type: $\chi > \epsilon$,
- (b) UF type: $|\chi| \leq \epsilon$,
- (c) CC type: $\chi < -\epsilon$. (9)

There is no prior knowledge to determine ϵ , but it can be chosen adaptively for empirical data. Here, one can take, for example, $\epsilon=0.025$, which corresponds to a tolerance of 5% from the probability $P=0.5$.

While actual phase distributions may show more intricate morphology, classification into the above three generic morphology types is in all cases possible at the first level of shape approximation. The output of the Hilbert transform of an IMF consists of one time series of amplitude and one time series of phase. This implies that the resultant time series of phase is equivalent to a measure performed on the “normalized” wave form obtained from renormalizing the original IMF by the time-varying amplitude. The information recorded in the original time series is then mainly stored in the time series of phase, and the physics of the system is thus imprinted in the phase structures. In ECG, the features characterized by the instantaneous phase are the variations of the profiles of electric potential. Phase statistics of an IMF performed in a specified window reflect the relative contents of the particular phase profiles present in the ECG potential curves. Uniform phase distribution implies regular sinusoidal waveforms throughout the sampling period, or all possible profiles taking place with the same probability, while non-uniform distributions correspond to particular waveforms (as

shown in Fig. 5), persisting for a significantly long period of time. Therefore, the various phase patterns noted above are associated with the persistence of the profiles shown in the time series in Fig. 5. Note that the first mode c_1 is close to zero in some intervals. This implies that small fluctuations are absent or smeared out in those epochs. For a curve close to zero, the waveform will be similar to the CC type in Fig. 5. This in turn implies the absence of high-frequency fluctuations contributed through the breakdown of multispiral waves. Furthermore, the CV type distribution implies myocardial cells are subjected for a longer time to more rapidly fluctuating electric potential than those of UF and CC types of distributions. Here, we remark that while the existence of high frequency fluctuations in the first component is essential and revealed in spectral analysis, the spectrum of this component is a narrow band which is usually not substantial enough for the classification. Consequently, the phase distribution is regarded as a tool, or a morphological probe, for inspecting the properties of conductance in the heart.

IV. RESULTS AND DISCUSSIONS

Next, we present an analysis of the data based on the phase statistics approach. As shown in Table I, some patients have more than one VTA intervals. For such cases, we calculate the registered VTA ECG intervals separately. The actual phase distribution plots for the first IMF c_1 of 28 VTA intervals for all the subjects are presented in the Appendix, together with the classifications based on Eq. (9). The statistics of the phase distribution patterns of first IMF c_1 and the VTA consequences are presented in Table I.

For comparison, we also calculated phase distributions of the second IMFs and third IMFs. Figure 6 shows the distributions of χ for the first IMFs, second IMFs and third IMFs of 28 VTA intervals. Note that in the figure, for a subject with more than one occurrence of VTA data, early VTAs are indicated by a solid triangle. For example, for nonsurvival

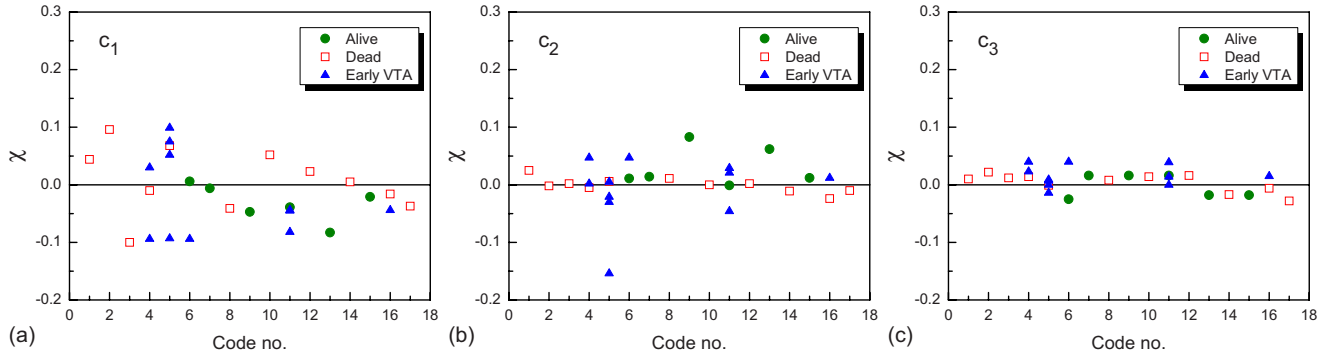


FIG. 6. (Color online) Distribution of χ for the first IMFs, second IMFs and third IMFs of 28 VTA intervals. For a subject having more than one occurrence of VTA data, his early VTA intervals are labeled with a solid blue triangle and the last VTA with an open red square (for nonsurvivor), and with a solid green circle (for survivor).

subject S_{05} , who had 5 VF data, the early 4 VF intervals are labeled with a solid, blue triangle and the last VF with an open, red square. Figure 6 shows that χ values of c_1 are better than χ values of c_2 and c_3 for differentiating survival and nonsurvival VTA patients. Thus, hereafter, we focus on the statistics of c_1 component.

By considering the correlation between the phase distribution patterns of the *last* VTA interval and the consequence of VTA, we conclude that the VTA with the CC pattern has a survival rate of 50%, the VTA with the UF pattern has a survival rate of 43%, and the VTA with the CV pattern has a survival rate of 0%. Note that the CV pattern is not observed in VTA ECGs other than VF, and the last VFs with the CV pattern were not self-terminated.

A self-terminating VF is not always an isolated phenomenon and may reoccur within a short period. Several subjects in our database (such as S_{04} , S_{05} , S_{06} , S_{11} , and S_{16}) have more than one VTA interval registered. The early VTAs contain information pertinent to the final outcome and should thus be taken into consideration in order to improve the predictive power of the method by learning from past self-termination of VTA. The statistics of the phase distribution patterns for *all* VTA intervals (including the early and the last VTA intervals) are presented in Table II. A VTA with CC pattern has a survival rate of 54%, a UF pattern has a survival rate of

43%, while a CV pattern has a survival rate of 0%, implying that the VTA (VF) with an early episode in the CV pattern can adumbrate a lethal outcome.

From the survey of the phase distribution patterns and VTA outcomes in the above statistics and Fig. 6, the largest χ of the first IMFs appears to be the worst condition for VTA patients. We then select the VTA interval with the largest χ among VTA intervals of a subject and denote it as VTA* for further statistical analysis. The simple statistics, presented in Table II, show that the CC type VTA has a survival probability of 60%, while the CV type VTA has 0% probability. We plot the distribution of the VTA* with respect to the corresponding consequences for 17 patients in Fig. 7. The survival probability (SP) as a function of χ is estimated by the logistic regression, and the curve of SP is determined by $SP(\chi) = e^{\alpha+\beta\chi} / (1 + e^{\alpha+\beta\chi})$ with $(\alpha = -0.795, \beta = -19.256)$, significance level of the fit $p = 0.180$ and significance level of model coefficients $p = 0.079$. The former is large enough for a reasonable fit, while the latter is marginal for an explicit classification of $p = 0.05$. For statistics of 17 samples, such significance levels should be acceptable. In the 17 VTA episodes, there are 6 survivors and 11 nonsurvivors. A rough estimate for a VTA is a survival rate of $6/17 = 35.3\%$. Figure

TABLE II. Correlation between phase distribution patterns of 17 last VTAs, all 28 VTA intervals, and VTA intervals with the largest χ (denoted by VTA*) among VTA intervals of each subject and the survival outcome.

Reference	Pattern	No. of cases	Survival	Nonsurvival
Last VTA	CC	6	3 (50%)	3 (50%)
	UF	7	3 (43%)	4 (57%)
	CV	4	0 (0%)	4 (100%)
All VTAs	CC	13	7 (54%)	6 (46%)
	UF	7	3 (43%)	4 (57%)
	CV	8	0 (0%)	8 (100%)
VTA*	CC	5	3 (60%)	2 (40%)
	UF	7	3 (43%)	4 (57%)
	CV	5	0 (0%)	5 (100%)

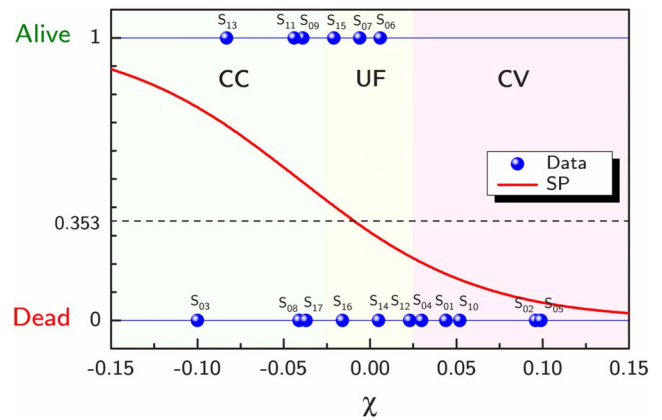


FIG. 7. (Color online) Distribution of VTA intervals with the largest χ among VTA intervals and the corresponding VTA outcomes of 17 patients. The survival probability SP is derived from the logistic regression. 0.353 is the overall survival rate for the 17 patients in the present data.



FIG. 8. (Color online) Summary of the phase distributions for the first IMF c_1 of 28 VTA intervals of 17 subjects. The colors green (dark) and red (unfilled) indicate the last VTA intervals, and blue (oblique) is for early VTA. Those with the color green (dark) are survivors, and those with the color red (unfilled) are nonsurvivors.

7 implies that the phase distribution patterns have a good correlation with the consequences of VTA (dead/alive outcome). Furthermore, survival probability SP in principle decreases monotonously with χ . Subjects with VTAs classified into the CV regime are nonsurvivors (i.e., SP lower than 35.3%). The statistics for the last VTAs and all VTAs leads to similar conclusions [36].

Note that the phase statistics can be dependent on the duration of VTA. In our study, the durations of the VTAs in Table I have a wide range, from being less than 10 s to more than 1500 s. Typically, a shorter duration may have too few data for statistics, and statistics on a longer duration can smear the temporal trend of phase distribution. To verify our statistics and to explore the temporal trend of the phase distribution, instead of using the full length of the VTA intervals for the analysis, we have also used a small window size to define time-dependent $\chi(t)$ by sliding the window on the time course of the VTAs. For instance, by using 30 s as a window, the evolution of $\chi(t)$ was calculated to detect the trend of the phase distribution in a VTA interval. The classification of VF discussed above was found to be substantially consistent with the temporal trend study, while no specific relationship between the evolution of $\chi(t)$ and the progression of VT into VF, or VF into VT was found. Furthermore, we have observed a typical scenario that $\chi(t)$ for nonsurvivors usually have the CV type distribution in VF, while $\chi(t)$ for survivors rarely enter into the regime of the CV type distribution [37]. Such an implementation is useful for further studies of the correlation between the phase distribution patterns and non-self-terminating VF. It may also have a potential application in real-time monitoring of the CV type VF.

V. CONCLUSIONS

In conclusion, we have investigated VTA time series by using the approach of phase distribution which has recently been developed to study financial [17] and physiological [18] time series, and found that CV type VF intervals adumbrate occurrences of non-self-terminating VF, which is also most probably the CV type. The physiological implications of the CV phase distribution patterns identified in this work as leading to death are explained by the persistence of high-frequency fluctuations of electric potential. This high-frequency component has not been seriously considered as a characteristic mode of VF in early studies, and has usually

been considered as noise. Instead, the mean-field component (lower frequency), corresponding to the c_3 mode in Fig. 2, has been addressed. It is known that the dominant frequency of VF signals increases during early VF and decreases as VF progresses as a result of progressive ischemia [32,38]. These observations are far from being conclusive or robust as they are obtained using only 17 data sets. Nevertheless, our study shows for the first time that the persistence of high-frequency fluctuations in ECG which leads to fatal outcome is a critical characteristic revealed in the phase distribution of the c_1 mode in Fig. 2, with an oscillatory frequency up to 25 Hz. The mechanism behind the complex activation sequences during VF has been a topic of intense research and a subject of much discussion and debate. At this point, we cannot clarify the high-frequency activation on the physiological bases. Further research focusing on animal studies and computer simulations of VF is required to associate possible mechanisms of VF with the CC and CV phase distribution patterns observed and reported here as the predominant attribute of non-self-terminating VF. Furthermore, more precise and quantitative analysis is also required to predict the progression of VT into VF, since the detection of VF onset is critical for ICD. The integration of the time-dependent $\chi(t)$ and evolution of the dominant frequency in VF is a theme of our future work.

ACKNOWLEDGMENTS

This work was supported by the National Science Council of the Republic of China (Taiwan) under Grants No. NSC 96-2112-M-008-021-MY3, No. 97-2627-B-008-004 (M.C.W.), No. 96-2911-M-001-003-MY3, and No. 98-2911-I-001-028 (C.K.H.), National Center for Theoretical Sciences in Taiwan, and (in part) by grants from the Medical and Welfare Equipment Laboratory, Japan, to Y.Y.

APPENDIX: NORMALIZED PHASE DISTRIBUTIONS OF FIRST IMFS OF VTA TIME SERIES

Figure 8 summarizes the phase distributions for the first IMF c_1 of 28 VTA intervals of 17 subjects. Here, we have used the color green for the last VTA data of survivors, and the color red for nonsurvivors. For a subject with more than one occurrence of VTA data, early VTA data are labeled with the color blue.

-
- [1] C.-K. Peng, S. V. Buldyrev, S. Havlin, M. Simons, H. E. Stanley, and A. L. Goldberger, *Phys. Rev. E* **49**, 1685 (1994).
 - [2] J. F. Muzy, E. Bacry, and A. Arnéodo, *Int. J. Bifurcat. Chaos* **4**, 245 (1994).
 - [3] A. Argoul, A. Arnéodo, G. Grasseau, Y. Gagne, E. J. Hopfinger, and U. Frisch, *Nature (London)* **338**, 51 (1989).
 - [4] A. Arnéodo, E. Bacry, S. Manneville, and J. F. Muzy, *Phys. Rev. Lett.* **80**, 708 (1998).
 - [5] K. Kiyono, Z. R. Struzik, N. Aoyagi, F. Togo, and Y. Yamamoto, *Phys. Rev. Lett.* **95**, 058101 (2005).
 - [6] A. Arnéodo, E. Bacry, P. V. Graves, and J. F. Muzy, *Phys. Rev. Lett.* **74**, 3293 (1995).
 - [7] P. C. Ivanov, L. Amaral, A. L. Goldberger, S. Havlin, M. G. Rosenblum, Z. R. Struzik, and H. E. Stanley, *Nature (London)* **399**, 461 (1999).
 - [8] C.-K. Peng, S. Havlin, H. E. Stanley, and A. L. Goldberger, *Chaos* **5**, 82 (1995).
 - [9] A. Arnéodo, N. Decoster, and S. G. Roux, *Phys. Rev. Lett.* **83**, 1255 (1999).
 - [10] N. Decoster, S. G. Roux, and A. Arnéodo, *Eur. Phys. J. B* **15**,

- 739 (2000).
- [11] A. Arnéodo, J. F. Muzy, and D. Sornette, *Eur. Phys. J. B* **2**, 277 (1998).
- [12] L. Laloux, P. Cizeau, J. P. Bouchaud, and M. Potters, *Phys. Rev. Lett.* **83**, 1467 (1999).
- [13] V. Plerou, P. Gopikrishnan, B. Rosenow, L. A. Nunes Amaral, and H. E. Stanley, *Phys. Rev. Lett.* **83**, 1471 (1999).
- [14] W.-J. Ma, C.-K. Hu, and R. E. Amritkar, *Phys. Rev. E* **70**, 026101 (2004).
- [15] K. Kiyono, Z. R. Struzik, and Y. Yamamoto, *Phys. Rev. Lett.* **96**, 068701 (2006).
- [16] N. E. Huang, Z. Shen, S. R. Long, M. C. Wu, H. H. Shih, Q. Zheng, N.-C. Yen, C.-C. Tung, and H. H. Liu, *Proc. R. Soc. London, Ser. A* **454**, 903 (1998).
- [17] M.-C. Wu, M.-C. Huang, H.-C. Yu, and T. C. Chiang, *Phys. Rev. E* **73**, 016118 (2006).
- [18] M.-C. Wu and C.-K. Hu, *Phys. Rev. E* **73**, 051917 (2006).
- [19] M.-C. Wu, *Physica A* **375**, 633 (2007).
- [20] M.-C. Wu, *J. Korean Phys. Soc.* **50**, 304 (2007).
- [21] D. P. Zipes *et al.*, *J. Am. Coll. Cardiol.* **48**, e247 (2006).
- [22] Z.-J. Zheng, J. B. Croft, W. H. Giles, and G. A. Mensah, *Circulation* **104**, 2158 (2001).
- [23] M. Josephson and H. J. J. Wellens, *Circulation* **109**, 2685 (2004).
- [24] S. B. Dunbar, *Am. J. Crit. Care* **14**, 294 (2005).
- [25] A. Kočańska, E. Lewicka-Nowak, and B. Zarzycka, *Folia Cardiol.* **13**, 171 (2006).
- [26] A. M. Gillis, *N. Engl. J. Med.* **351**, 2540 (2004).
- [27] H. J. J. Wellens, A. P. Gorgels, and H. de Munter, *Circulation* **107**, 1948 (2003).
- [28] K. Nair, K. Umapathy, E. Downar, and K. Nanthakumar, *Heart Rhythm* **5**, 1198 (2008).
- [29] G. K. Moe, W. C. Rheinboldt, and J. A. Abildskov, *Am. Heart J.* **67**, 200 (1964).
- [30] A. V. Zaitsev, O. Berenfeld, S. F. Mironov, J. Jalife, and A. M. Pertsov, *Circ. Res.* **86**, 408 (2000).
- [31] P. G. Milner, *Am. J. Cardiol.* **56**, 588 (1985).
- [32] M. P. Nash, A. Mourad, R. H. Clayton, P. M. Sutton, C. P. Bradley, M. Mayward, D. J. Paterson, and P. Taggart, *Circulation* **114**, 536 (2006).
- [33] D. J. Christini and L. Glass, *Chaos* **12**, 732 (2002).
- [34] N. Bursac, F. Aguel, and L. Tung, *Proc. Natl. Acad. Sci. U.S.A.* **101**, 15530 (2004).
- [35] J. N. Weiss, Z. Qu, P.-S. Chen, S.-F. Lin, H. S. Karagueuzian, H. Hayashi, A. Garfinkel, and A. Karma, *Circulation* **112**, 1232 (2005).
- [36] If the last VTAs and all VTAs are considered, we have $\alpha = -0.840$, $\beta = -18.431$ with significance level of fit $p = 0.159$ and significance level of model coefficients $p = 0.108$ for the last VTAs, and $\alpha = -0.975$, $\beta = -18.057$, significance level of fit $p = 0.055$ and significance level of model coefficients $p = 0.020$ for all VTAs.
- [37] M.-C. Wu, Z. R. Struzik, E. Watanabe, Y. Yamamoto, and C.-K. Hu, *AIP Conf. Proc.* **922**, 573 (2007).
- [38] P. S. Chen, T. J. Wu, C. T. Ting, H. S. Karagueuzian, A. Garfinkel, S.-R. Lin, and J. N. Weiss, *Circulation* **108**, 2298 (2003).